Journal of Non-Crystalline Solids 565 (2021) 120841

Contents lists available at ScienceDirect

Journal of Non-Crystalline Solids

journal homepage: www.elsevier.com/locate/jnoncrysol

In-situ observations on shear-banding process during tension of a Zr-based bulk metallic glass composite with dendrites

G.H. Duan [a,b], M.Q. Jiang [b,c], X.F. Liu [b,c], L.H. Dai [b,c], J.X. Li [a,*]

[a] Corrosion and Protection Center, University of Science and Technology Beijing, Beijing 100083, China
[b] State Key Laboratory of Nonlinear Mechanics, Institute of Mechanics, Chinese Academy of Sciences, Beijing 100190, China
[c] School of Engineering Science, University of Chinese Academy of Sciences, Beijing 100049, China

ARTICLE INFO

Keywords:
Metallic glass composite
In-situ tension
Shear band
Tensile failure

ABSTRACT

In-situ quasistatic tension experiments inside scanning electron microscope were performed to study shear-banding behaviors of a Zr-based bulk metallic glass composite with the 50% volume fraction of dendritic phases. It was observed that the shear band initiates at the interface of metallic glass matrix and dendrites, and then propagates in the glass matrix. Dendrites change the propagation direction of shear bands or terminate the shear band within them. Both modes facilitate the multiplication of shear bands in the glass matrix between dendrites. Upon further loading, shear bands preferentially develop into cracks in the matrix, but the dendrites significantly improve the crack resistance. This work provides the first-hand information of shear-banding and failure of the Zr-based metallic glass composite with dendrites.

1. Introduction

The lack of long-range order endues metallic glasses (MGs) with unique mechanical behaviors [1–3]. The room-temperature plastic deformation of MGs is usually dominated by a single or limited number of shear bands [4–6], which usually incur catastrophic failure with macroscopic brittleness. Various methods [7–15] have been developed to improve global plasticity of MGs. Among these methods, introducing in situ crystalline phases into MG matrix to form composites is proved to be effective [16–21]. These in situ crystalline phases can be either B2 or dendritic phases. Upon loading, the B2 phases usually undergo martensitic transformation [7] or twinning [9,22] to contributing the global plasticity of composites. Furthermore, by in-situ scanning electron microscopy (SEM) tensions, Jiang et al. [23] have revealed that Youngs' modulus and volume fraction of B2 phases can significantly affect shear band behaviors in MG matrix and thus turn the tensile ductility. In MG matrix composites with in-situ dendrites, both multiple shear bands in matrix and deformation bands or dislocations in dendrites contribute to the plastic deformation. In the past decades, extensive efforts [18–21,24–26] have been made to optimize the trade-off between the strength and plasticity or ductility of the composites by modifying chemical components and topological structures of both dendritic phases and MG matrix. In the aspect of deformation mechanism, it is well accepted that dendritic phases facilitate nucleation of shear bands at their interfaces with the glass matrix, and meanwhile act as obstacles to fast propagation of shear bands. In a Ti-based MG composite with dendrites, Qiao et al. [21] have found that fragmentation of dendrites induced by multiple shear bands is responsible for the high tensile ductility of the composite. Very recently, combining digital image correlation method with finite element analysis, Liu et al. [27] have studied the strain filed evolution and shear banding of a Zr-based MG matrix composite with in-situ dendrites. However, the precise shear-band process in this type of composites still remains unclear due to the limited spatial resolution, whereas in-situ microtests inside SEM provide such possibility [23,28].

In this work, we perform an in-situ tension of a Zr-based MG matrix composite containing homogeneously distributed dendrites under a quaistatic strain rate. We focus on effects of dendritic phases and their interfaces with glass matrix on the initiation and multiplication of shear bands, which can provide direct evidence for the deformation and failure mechanism of this composite under tension. Here, we perform tension tests because the tensile ductility is more important than compressive plasticity, but meanwhile is difficultly achieved.

* Corresponding author.
E-mail address: jxli65@ustb.edu.cn (J.X. Li).

https://doi.org/10.1016/j.jnoncrysol.2021.120841
Received 31 December 2020; Received in revised form 22 March 2021; Accepted 31 March 2021
Available online 12 April 2021

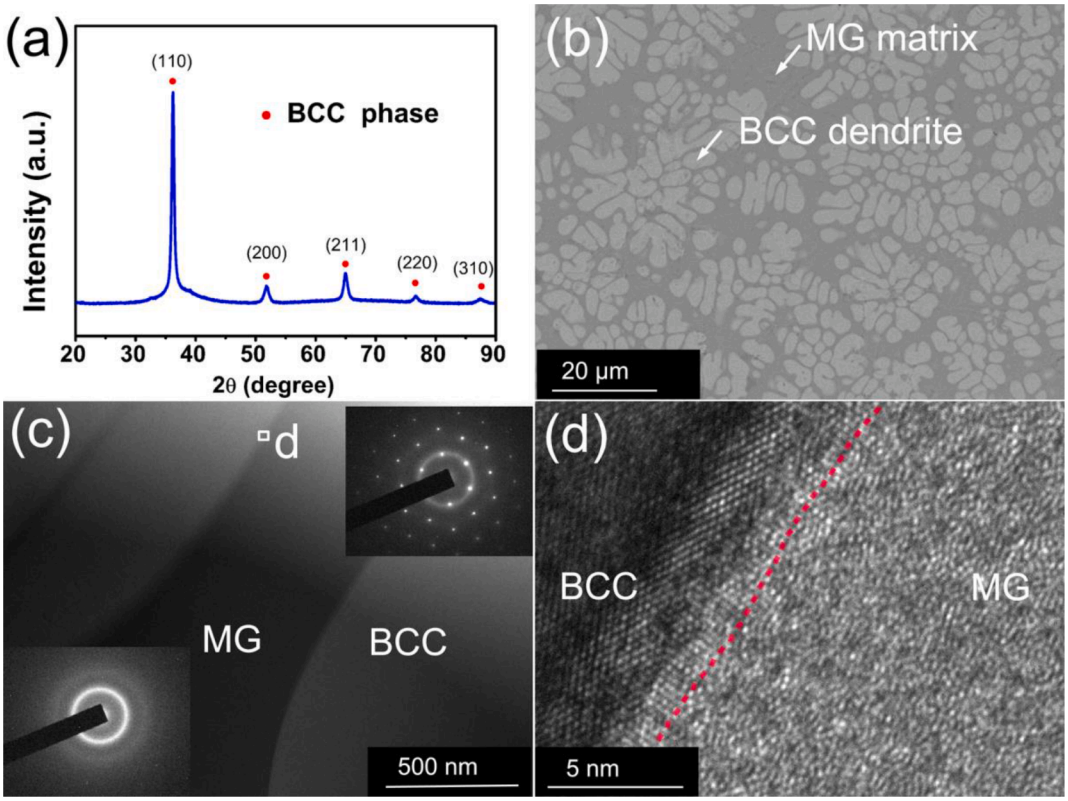

Fig. 1. The structural and phase characterizations of the as-cast MG composite with dendrites. (a) XRD profile, (b) TEM image, (c) TEM image, and (d) HRTEM image. Insets of (c) are the corresponding SAED patterns

2. Experimental procedure

A typical MG composite with nominal components [29], $Zr_{60}Ti_{12}Nb_8Ni_{4.5}Cu_{5.5}Be_{10}$ (at. %), was adopted as the model material. Master ingots of this composite were prepared by arc melting the mixture of high purity Zr, Ti, Nb, Cu, Ni and Be with a purity higher than 99.9% under the protection of a Ti-gettered argon atmosphere. The ingots were remelted at least 5 times and then suctioned into a copper mold. The as-cast plates have a dimension of about 60 × 20 × 2 mm^3. The phases and structures of the as-cast composites were checked by X-ray diffraction (XRD, Rigaku Smartlab 9) using CuKα radiation with a step size of 0.02°, high revolution transmission electron microscope (HRTEM, FEI G20) and SEM (FEI Sirion400nc).

The as-cast plate was machined into dog-bone shaped specimens for tensions. The dimension of the gauge section is 3 × 1.5 × 1 mm^3. Then single edge notch of 0.2 mm in width and 0.5 mm in depth was cut by tungsten filament at the center of the tensile specimens to ensure that the deformation occur at the middle region of the specimens. All specimens were mechanically ground and carefully polished in 1 μm diamond suspension, and then electro-etched by an alcohol solution containing 5% volume fraction of $HClO_4$. The in-situ tensile tests were carried out by the FEI Sirion400nc with the Gatan Microtest2000 tensile stage. The tests were performed at room temperature with a displacement rate of 0.1 mm/min. We repeated 6 tests, but only show a representative one.

3. Results and discussion

3.1. Morphology and tension property

Fig. 1(a) shows the XRD profile of the as-cast MG composite. It can be seen that the sharp peaks of the body-centered cubic (BCC) crystalline phase are superimposed on the broad diffuse scattering maximum of the

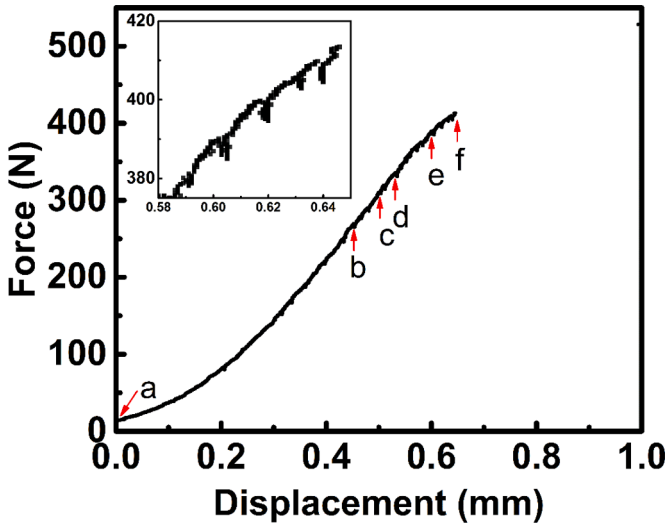

Fig. 2. The force-displacement curve of the composite under the quasi-static tension.

metallic glass matrix with the amorphous structure. The microstructural morphology and phase structures of this composite are further checked by SEM (Fig. 1(b)) and HRTEM (Fig. 1(c and d)) observations. As shown in Fig. 1(b), the dark area is the MG matrix, and the light colored phases are the BCC dendrites. The individual dendrite size is about 50 μm and the secondary branches are 4.7±1.7 μm in length. These dendrites are homogeneously distributed in the matrix. The volume fraction of dendrites is estimated to be about 50%. Fig. 1(c) shows the TEM image of both MG and BCC dendrites, and the insets are their corresponding selected-area electron diffraction (SAED) patterns. Fig. 1(d) shows the

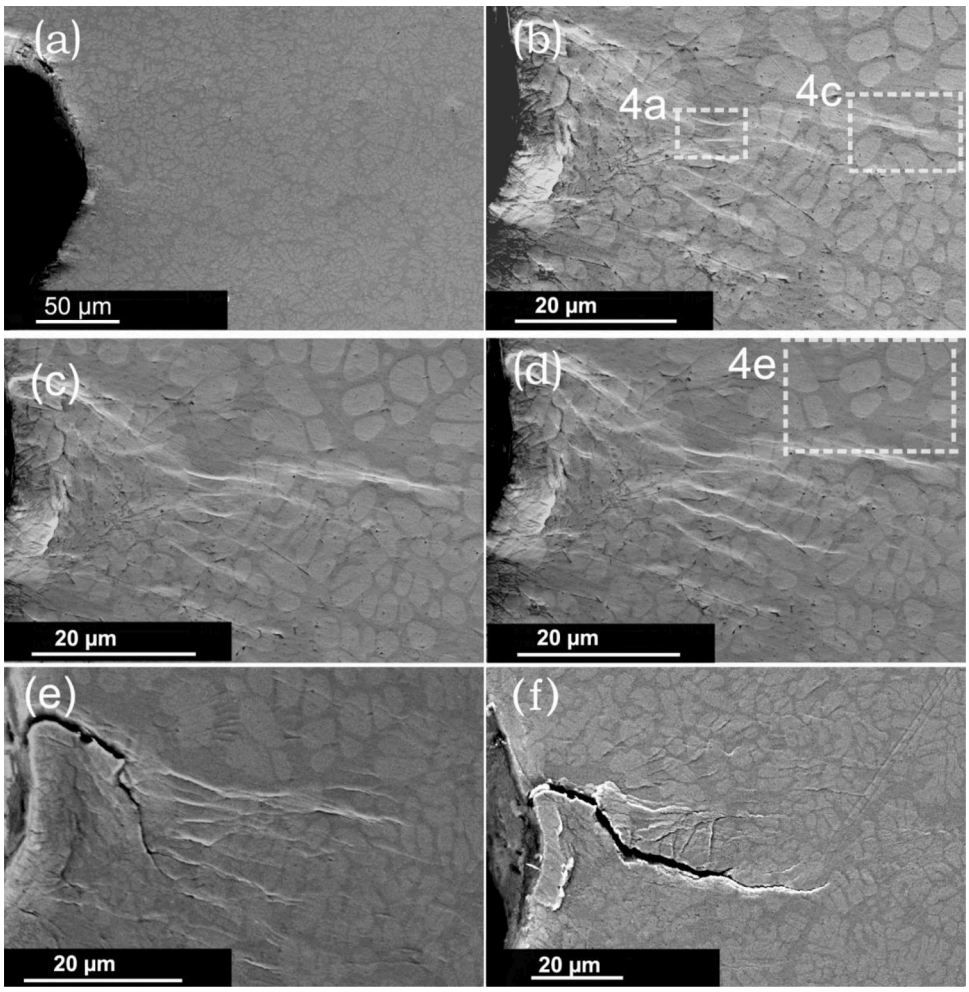

Fig. 3. SEM morphologies on the processes of shear bands and crack propagation of $Zr_{60}Ti_{12}Nb_8Ni_{4.5}Cu_{5.5}Be_{10}$ single edge notched specimen by in-situ tension. (a)–(f) correspond to the six stop stages of macroscopic deformation, as marked by red arrows in Fig. 2.

HRTEM image of a region marked by 'd' in Fig. 1(c). It is clear to see an interface between the MG matrix and a crystalline dendrite. These observations are consistent with the previous study [18].

The representative force-displacement of the MG composite under in-situ SEM tension is shown in Fig. 2. It can be seen that this composite undergoes a deformation displacement of about 0.6 mm, and eventually fails at a loading of about 413N. The corresponding fracture strain and strength are about 21.5% and 929 MPa, respectively. Compared to typical pure MGs [30], the composite generally shows a certain tensile ductility. This is further evidenced by the flow serration appearing in the stress-strain curve (the inset of Fig. 2). The serrated flow usually implies multiplication of shear bands in samples [31], rather than a single, dominated one.

3.2. In-situ observation of shear bands

In order to in-situ obverse shear bands, we stop the tensile loading at different stages that are marked by the red arrows in Fig. 2. Fig. 3(a–f) shows the shear bands and cracks corresponding to the six stop stages, where we focus on the region in front of the notch tip. It is indeed seen that multiple shear bands dominate the plastic deformation. These shear bands nucleate at the notch tip or the interfaces between the matrix and the dendrites. The former offers relatively low nucleation energy for shear-banding instability. For the latter, there is remarkable stress concentration due to a mismatch of structure and property between the matrix and the dendrites. The stress concentration also facilitates the shear-banding instability. After that, shear bands will preferentially propagate in the MG matrix. This is because that the shear band toughness in the MG is much lower than that of the soft dendrites [32]. The shear-band toughness is a physical quantity that measures the critical plastic energy dissipated in a shear band from its initiation to termination before cracking. Lower shear-band toughness implies the relatively easy propagation of shear bands in materials. This concept was originally proposed by Grady and Kipp [33,34], and later was introduced to MGs or their composites by some of us [5,32]. According to our previous study of a composition-similar Zr-based BMG with dendrites [32], the shear-band toughness of MG matrix is of the order of 10^0–10^1 $MPam^{1/2}$, while the soft dendrites have the shear-band toughness of about 10^2 $MPam^{1/2}$.

Fig. 4(a and b) shows the enlarged views of the local area marked by '4a' in Fig. 3(b). It is very clear to observe that a shear band 'S1' initiates in the MG matrix at its interface with a dendrite 'D1'. Upon loading, this 'S1' shear band propagates in the matrix until it encounters another dendrite 'D2'. Then the shear band bends at the boundary and causes lamellar slip deformation in the 'D2' dendrite. Similar behavior is also observed for the shear band 'S2'. The nucleation mode of shear bands observed in the present composite is very different from the observation by Huang et al [26]. They found that shear bands first nucleate in dendritic phases of a ZrTi-based MG composite. The possible reason is the very small distance between dendrites due to the higher volume fraction and smaller sizes. Actually the nucleation of shear bands becomes relatively difficult in MGs with smaller characteristic sizes

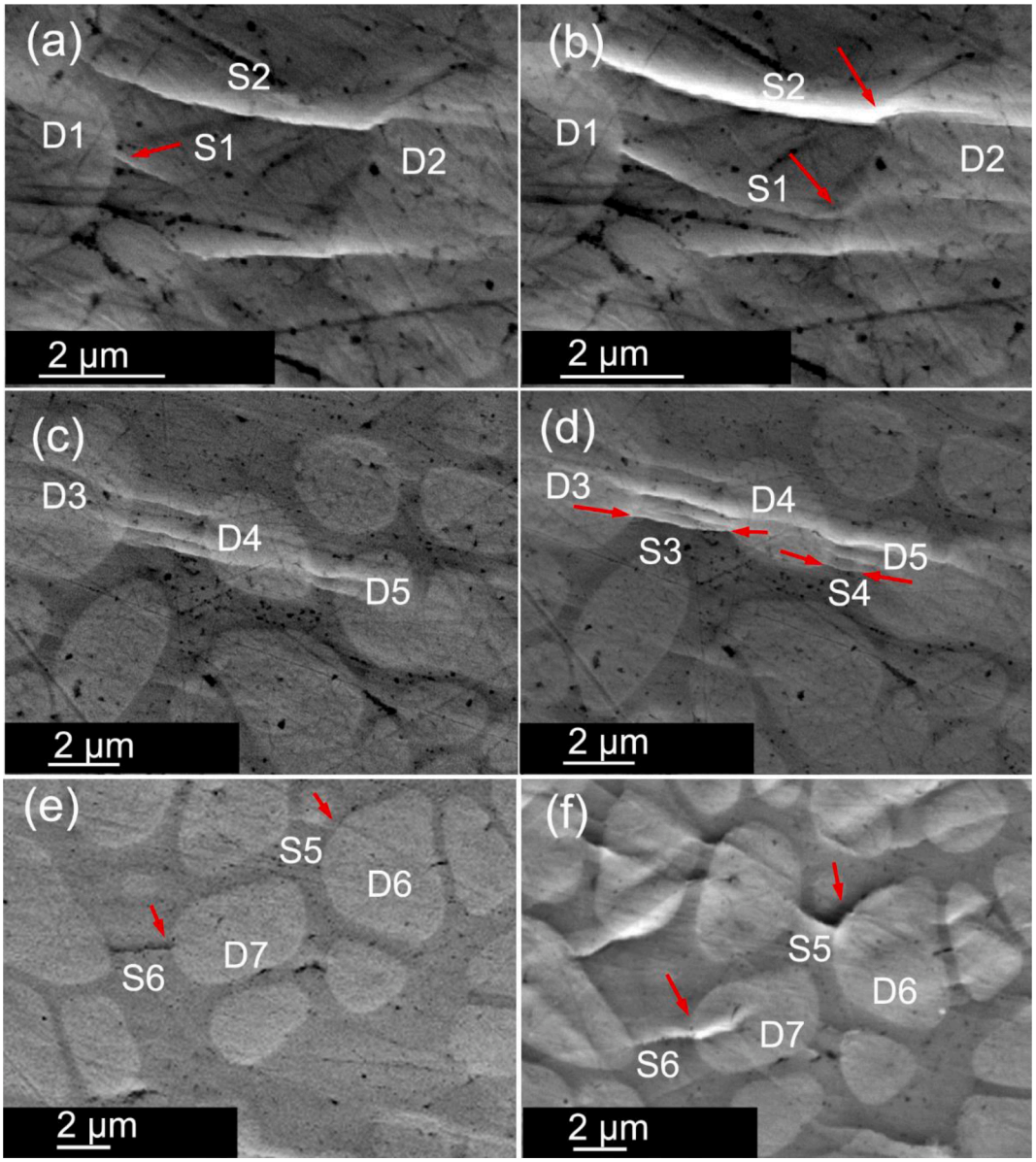

Fig. 4. In-situ SEM observations of shear bands. (a and b) corresponds to a local region marked by '4a' in Fig. 3(b), (c and d) corresponds to a local region marked by '4c' in Fig. 3(b), and (e and f) corresponds to a local region marked by '4d' in Fig. 3(b)

[35–37]. Fig. 4(c and d) shows the enlarged views of the local area marked by '4c' in Fig. 3(b). The multiplication of shear bands can be observed in the MG matrix between two dendrites. For example, the shear band 'S3' is a new one that is formed between the dendrites 'D3' and 'D4'. Another new shear band 'S4' is formed between the dendrites 'D4' and 'D5'. Fig. 4(e and f) shows the enlarged views of the local area marked by '4e' in Fig. 3(d). We observe two different modes how a shear band is blocked by the dendrite. The first mode can refer to the shear band 'S5'. Its propagation is stopped by the dendrite 'D6'. With further deformation, this shear band changes its direction and propagates along the boundary between the matrix and the dendrite. The second mode is exemplified by the shear band 'S6'. After it reaches the dendrite 'D7', this shear band enters the dendrite. Significant plastic deformation occurs within this dendrite. The 'S6' shear band ultimately terminates in the 'D7' dendrite. The two block-modes of shear bands by dendrites should dissipate much plastic work, thus contributing to the macroscopic ductility. In addition, the strong interaction between shear bands and dendrites will redistribute the stress and strain fields in the composite, and further affects the modulus or hardness of both phases. This issue deserves further study in the future work.

3.3. Fracture features

Fig. 5(a) shows morphology of the sample surface near the main crack plane of this composite after final fracture. As magnified in Fig. 5 (b and c), there are many multiple shear bands accompanying the main crack. According to contrast of both phases in SEM, dendrites 'D8-D11' can be identified, as marked in Fig. 5(c). These dendrites ultimately fail by shear-band-induced cracks. We can see that there are many lamella cracks in the dendrites 'D8' and 'D9', although the two dendrites still maintain integrity. These cracks should be induced by propagation of shear bands around the dendrite. The dendrites 'D10' and 'D11' lose the integrity, because they are passed through by the main crack.

Fig. 6 presents the fracture patterns of main crack plane of the composite. From Fig. 6(a), we can see that the fracture surface is obviously divided into three zones: smooth slip-shear zone, river-like plastic zone and dimple-characterized fracture zone. The typical characteristics of the three zones are shown in Fig. 6(b–d), respectively. The smooth

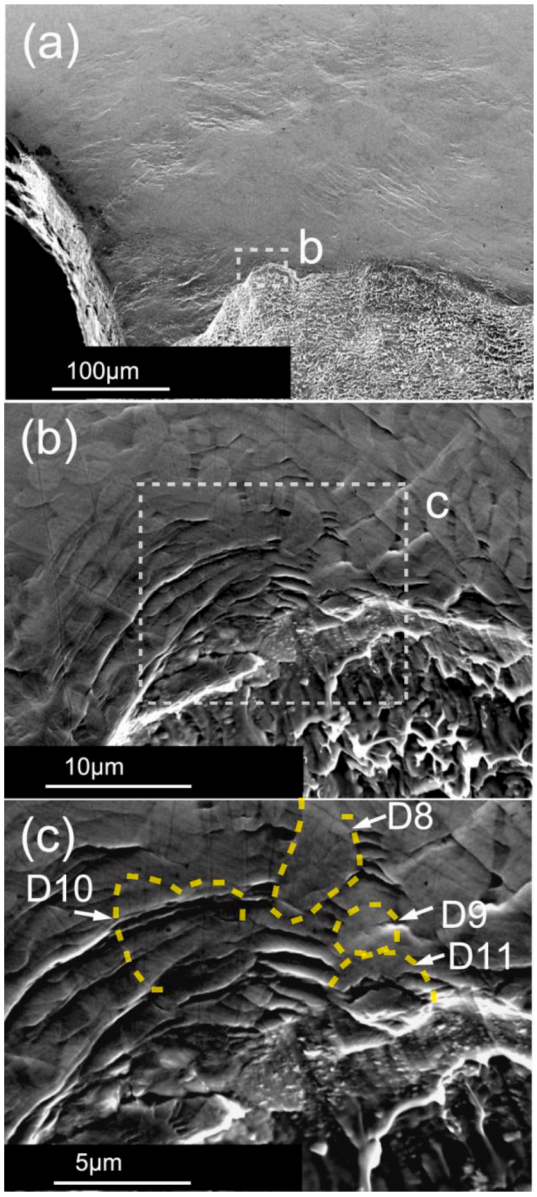

Fig. 5. (a) Morphologies of sample surface near the main crack of the composite, (b) and (c) the enlarged views of local regions marked by 'b' in (a) and by 'c' in (b), respectively.

shear lip area is near the sample surface and closely connected with the shear band propagation. The following two zones are formed due to the shear-band-induced cracking. Rough veins are the typical fracture patterns. These vein patterns become much rougher and deeper along the cracking direction, indicating the high resistance to fracture [38]. The observed vein patterns in this composite are very different from the flower-like patterns during fracture of the pure Zr-based MGs under quasistatic tensions [30,39,40]. In the latter, the facture is usually dominated by single shear band, whereas in the present composite multiple shear bands control the final failure. In Fig. 6(d), equiaxed dimples with small cavities occupy the central region of the fracture surface. Both deep vein patterns and dimple provide solid evidence that the dendrites have interrupted the propagation of shear bands and increase tensile ductility of the composite [41,42].

4. Conclusions

The shear-banding behaviors in a Zr-based bulk metallic glass composite with dendrites are observed by in-situ SEM tension. It is found that shear band preferentially nucleate at the interface between the glass matrix and dendrites, and then propagate into the matrix. There are two different modes of how dendrites block the shear bands. In the first mode, dendrites alter the propagation direction of shear bands that propagate along the boundary between the matrix and dendrites. The second block mode is that shear band in the glass matrix terminate in dendrites. In addition, the existence of dendrites significantly improves the crack resistance, which is evidenced by deep vein patterns and rough dimples observed on the main crack surface.

CRediT authorship contribution statement

G.H. Duan: Conceptualization, Methodology, Investigation, Writing – original draft, Writing – review & editing. **M.Q. Jiang:** Formal analysis, Writing – review & editing. **X.F. Liu:** Writing – review & editing. **L. H. Dai:** Conceptualization, Methodology. **J.X. Li:** Conceptualization, Methodology, Writing – review & editing, Supervision.

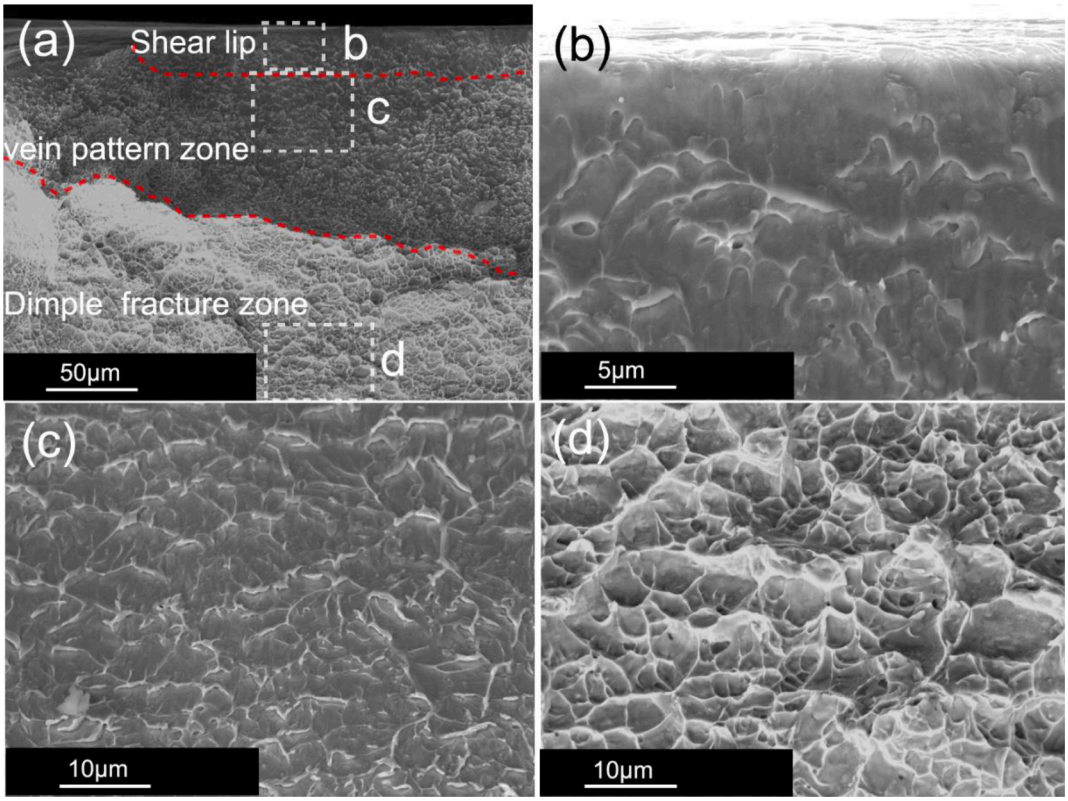

Fig. 6. (a) Tensile fracture surface of the composite, showing three characteristic zones: (b) smooth slip-shear zone, (c) river-like plastic zone and (d) dimple-characterized fracture zone. (b–d) corresponds to local regions marked by 'b-c', respectively.

Declaration of Competing Interest

The authors declare that they have no known competing financial interests or personal relationships that could have appeared to influence the work reported in this paper.

Acknowledgment

This work was supported by the National Natural Science Foundation of China (NSFC) Basic Science Center for "Multiscale Problems in Nonlinear Mechanics" (No. 11988102) and the NSFC (Grant Nos. 11972345, U1760203).

References

[1] C.A. Schuh, T.C. Hufnagel, U. Ramamurty, Mechanical behavior of amorphous alloys, Acta Mater. 55 (2007) 4067–4109.
[2] M.M. Trexler, N.N. Thadhani, Mechanical properties of bulk metallic glasses, Prog. Mater. Sci. 55 (2010) 759–839.
[3] W.H. Wang, Correlations between elastic moduli and properties in bulk metallic glasses, J. Appl. Phys. 99 (2006), 093506.
[4] M.Q. Jiang, L.H. Dai, On the origin of shear banding instability in metallic glasses, J. Mech. Phys. Solids 57 (2009) 1267–1292.
[5] M.Q. Jiang, L.H. Dai, Shear-band toughness of bulk metallic glasses, Acta Mater. 59 (2011) 4525–4537.
[6] A.L. Greer, Y.Q. Cheng, E. Ma, Shear bands in metallic glasses, Mater. Sci. Eng. R 74 (2013) 71–132.
[7] Y. Wu, Y.H. Xiao, G.L. Chen, C.T. Liu, Z.P. Lu, Bulk metallic glass composites with transformation-mediated work-hardening and ductility, Adv. Mater. 22 (2010) 2770–2773.
[8] M.D. Demetriou, M.E. Launey, G. Garrett, J.P. Schramm, D.C. Hofmann, W. L. Johnson, R.O. Ritchie, A damage-tolerant glass, Nat. Mater. 10 (2011) 123–128.
[9] S. Pauly, S. Gorantla, G. Wang, U. Kuhn, J. Eckert, Transformation-mediated ductility in CuZr-based bulk metallic glasses, Nat. Mater. 9 (2010) 473–477.
[10] Z.T. Wang, J. Pan, Y. Li, C.A. Schuh, Densification and strain hardening of a metallic glass under tension at room temperature, Phys. Rev. Lett. 111 (2013), 135504.
[11] C. Jeon, C.P. Kim, S.H. Joo, H.S. Kim, S. Lee, High tensile ductility of Ti-based amorphous matrix composites modified from conventional Ti–6Al–4V titanium alloy, Acta Mater. 61 (2013) 3012–3026.
[12] E.W. Huang, J. Qiao, B. Winiarski, W.-J. Lee, M. Scheel, C.-P. Chuang, P.K. Liaw, Y.-C. Lo, Y. Zhang, M. Di Michiel, Microyielding of core-shell crystal dendrites in a bulk-metallic-glass matrix composite, Sci. Rep. 4 (2014) 4394.
[13] S.V. Ketov, Y.H. Sun, S. Nachum, Z. Lu, A. Checchi, A.R. Beraldin, H.Y. Bai, W. H. Wang, D.V. Louzguine-Luzgin, M.A. Carpenter, A.L. Greer, Rejuvenation of metallic glasses by non-affine thermal strain, Nature 524 (2015) 200–203.
[14] Y.F. Cao, X. Xie, J. Antonaglia, B. Winiarski, G. Wang, Y.C. Shin, P.J. Withers, K. A. Dahmen, P.K. Liaw, Laser shock peening on Zr-based bulk metallic glass and its effect on plasticity: experiment and modeling, Sci. Rep. 5 (2015) 10789.
[15] J. Pan, Y.P. Ivanov, W.H. Zhou, Y. Li, A.L. Greer, Strain-hardening and suppression of shear-banding in rejuvenated bulk metallic glass, Nature 578 (2020) 559–562.
[16] D.C. Hofmann, J.Y. Suh, A. Wiest, G. Duan, M.L. Lind, M.D. Demetriou, W. L. Johnson, Designing metallic glass matrix composites with high toughness and tensile ductility, Nature 451 (2008) 1085–1089.
[17] J.W. Qiao, H.L. Jia, P.K. Liaw, Metallic glass matrix composites, Mater. Sci. Eng. R 100 (2016) 1–69.
[18] X.F. Liu, Y. Chen, M.Q. Jiang, P.K. Liaw, L.H. Dai, Tuning plasticity of in-situ dendrite metallic glass composites via the dendrite-volume-fraction-dependent shear banding, Mater. Sci. Eng. A 680 (2017) 121–129.
[19] Z. Liu, R. Li, G. Liu, W. Su, H. Wang, Y. Li, M. Shi, X. Luo, G. Wu, T. Zhang, Microstructural tailoring and improvement of mechanical properties in CuZr-based bulk metallic glass composites, Acta Mater. 60 (2012) 3128–3139.
[20] M.L. Lee, Y. Li, C.A. Schuh, Effect of a controlled volume fraction of dendritic phases on tensile and compressive ductility in La-based metallic glass matrix composites, Acta Mater. 52 (2004) 4121–4131.
[21] J.W. Qiao, A.C. Sun, E.W. Huang, Y. Zhang, P.K. Liaw, C.P. Chuang, Tensile deformation micromechanisms for bulk metallic glass matrix composites: From work-hardening to softening, Acta Mater. 59 (2011) 4126–4137.
[22] Y. Wu, D.Q. Zhou, W.L. Song, H. Wang, Z.Y. Zhang, D. Ma, X.L. Wang, Z.P. Lu, Ductilizing bulk metallic glass composite by tailoring stacking fault energy, Phys. Rev. Lett. 109 (2012), 245506.
[23] S. Jiang, S. Guo, Y. Huang, Z. Ning, P. Xue, W. Ru, J. Zhang, J. Sun, In situ study of the shear band features of a CuZr-based bulk metallic glass composite, Intermetallics 112 (2019), 106523.
[24] R.L. Narayan, P.S. Singh, D.C. Hofmann, N. Hutchinson, K.M. Flores, U. Ramamurty, On the microstructure–tensile property correlations in bulk metallic glass matrix composites with crystalline dendrites, Acta Mater. 60 (2012) 5089–5100.
[25] H. Zhou, S. Qu, W. Yang, An atomistic investigation of structural evolution in metallic glass matrix composites, Int. J. Plast. 44 (2013) 147–160.

[26] Y.J. Huang, J.C. Khong, T. Connolley, J. Mi, Understanding the deformation mechanism of individual phases of a ZrTi-based bulk metallic glass matrix composite using in situ diffraction and imaging methods, Appl. Phys. Lett. 104 (2014), 031912.
[27] X.F. Liu, Y. Chen, L.H. Dai, Deformation field evolution and shear banding of an in-situ crystal reinforced amorphous alloy composite, Sci. China Phys. Mech. Astron. 50 (2020), 067006.
[28] H.J. Yang, J.W. Qiao, S. Wang, Y. Zhang, In-situ tension of dendrite-reinforced Zr-based metallic-glass-matrix composites, Acta Metall. Sin. 27 (2014) 621–626.
[29] F. Szuecs, C.P. Kim, W.L. Johnson, Mechanical properties of ZrTiNbCuNiBe ductile phase reinforced bulk metallic glass composite, Acta Mater. 49 (2001) 1507–1513.
[30] M.Q. Jiang, Z. Ling, J.X. Meng, L.H. Dai, Energy dissipation in fracture of bulk metallic glasses via inherent competition between local softening and quasi-cleavage, Philos. Mag. 88 (2008) 407–426.
[31] B.A. Sun, H.B. Yu, W. Jiao, H.Y. Bai, D.Q. Zhao, W.H. Wang, Plasticity of ductile metallic glasses: a self-organized critical state, Phys. Rev. Lett. 105 (2010), 035501.
[32] J.H. Chen, M.Q. Jiang, Y. Chen, L.H. Dai, Strain rate dependent shear banding behavior of a Zr-based bulk metallic glass composite, Mater. Sci. Eng. A 576 (2013) 134–139.
[33] D.E. Grady, M.E. Kipp, The growth of unstable thermoplastic shear with application to steady-wave shock compression in solids, J. Mech. Phys. Solids 35 (1987) 95–118.
[34] D.E. Grady, Properties of an adiabatic shear-band process zone, J. Mech. Phys. Solids 40 (1992) 1197–1215.
[35] D. Jang, J.R. Greer, Transition from a strong-yet-brittle to a stronger-and-ductile state by size reduction of metallic glasses, Nat. Mater. 9 (2010) 215–219.
[36] L. Tian, Y.Q. Cheng, Z.W. Shan, J. Li, C.C. Wang, X.D. Han, J. Sun, E. Ma, Approaching the ideal elastic limit of metallic glasses, Nat. Commun. 3 (2012) 609.
[37] Y. Chen, M.Q. Jiang, L.H. Dai, Collective evolution dynamics of multiple shear bands in bulk metallic glasses, Int. J. Plast. 50 (2013) 18–36.
[38] J.W. Qiao, P. Feng, Y. Zhang, Q.M. Zhang, G.L. Chen, Quasi-static and dynamic deformation behaviors of Zr-based bulk metallic glass composites fabricated by the Bridgman solidification, J. Alloys Compd. 486 (2009) 527–531.
[39] M.Q. Jiang, G. Wilde, J.H. Chen, C.B. Qu, S.Y. Fu, F. Jiang, L.H. Dai, Cryogenic-temperature-induced transition from shear to dilatational failure in metallic glasses, Acta Mater. 77 (2014) 248–257.
[40] J.X. Li, G.B. Shan, K.W. Gao, L.J. Qiao, W.Y. Chu, In situ SEM study of formation and growth of shear bands and microcracks in bulk metallic glasses, Mater. Sci. Eng. A 354 (2003) 337–343.
[41] C. Jeon, M.C. Jo, J. Lee, E.S. Park, J. Park, S.Y. Shin, Improvement of mechanical properties of Zr-based bulk amorphous alloys by high temperature heat treatment, Met. Mater. Int. 26 (2019) 1144–1151.
[42] Y.Y. Liu, P.Z. Liu, J.J. Li, P.K. Liaw, F. Spieckermann, D. Kiener, J.W. Qiao, J. Eckert, Universally scaling Hall-Petch-like relationship in metallic glass matrix composites, Int. J. Plast. 105 (2018) 225–238.